ISEC 2026 – 4th International Sustainable Energy Conference
Emerging Energy Technologies and System Integration
https://doi.org/10.52825/isec.v2i.3343

Published: 19 May 2026

Grid-Forming Controllers in the Distribution Network Landscape

Andres Tarraso[1,*], Maximillian Prasser[2], and Adolfo Anta[1]

[1]Austrian Institute of Technology GmbH

[2]Energinetze Steiermark

*Correspondence: Andres Tarraso, andres.tarraso-martinez@ait.ac.at

Abstract. The rapid expansion of renewable capacity is reshaping the power system landscape by introducing new actors into play, such as prosumers and energy communities, that would play a key role in the stability of the network under the distribution system landscape. This acceleration in the deployment of PV, wind and battery systems is leading to an extended use of advanced control strategies that mitigate the loss of inertia, flexibility and support towards the grid, so-called grid-forming (GFM) control. The decline of conventional synchronous generators has reduced native system inertia, leaving networks, both at the transmission and distribution levels, more vulnerable to instability. This reduces massively the time available for actuation to avoid escalated fault scenarios. In this regard, GFM technology offers a potential solution for synthetic inertia emulation and dynamic support for both voltage and frequency deviations, making it a key tool for enhancing stability in renewable-dominated distribution networks of the future. However, large-scale deployment increases the risk of oscillations and uncontrolled interactions due to voltage regulators and synchronization mechanisms or islanding procedures. The paper aims to address these challenges by developing a step-by-step analysis to ensure a safe, reliable and coordinated integration of distributed GFM resources in future power systems, validating them in realistic distribution network environments.

Keywords: Grid Forming, Inertia Emulation, Virtual Impedance, Grid Strength

1. Introduction

The rapid growth of photovoltaic (PV) installations, estimated to be about ~320 GW by 2025 and projected to reach a capacity close to the 600 GW by 2030 [1], has transformed the electrical landscape introducing new market participants into the electrical network scenario. These include households that both produce and consume electricity from the grid, with the capacity to provide grid-support and flexibility services, thereby strengthening the operational reliability of the network. In Europe, energy communities and microgrids have significantly advanced in efficiency and use of energy, largely due to the integration of power electronic converters and the smart deployment of battery energy storage systems. However, the overall poor management of renewable generation systems poses risks to the electrical network stability, which has been already seen in some failures in Australia and the U.S, and even in more severe cases, in the national blackout in Spain. In addition to this, the growing adoption of electric transportation increases the stress on the network. The integration of mobile loads that can create daily demand fluctuations depending on charging patterns is one of the key challenges. Some mitigation was established by the integration of battery storage capacity, that in some cases has exceeded the 20 GWh installation of battery energy in one year. Those systems can absorb excess energy during peak supply, allowing for some alleviation of variability in the power responses. However, with this massive integration and the removal of synchronous generators the power system has experienced a continuous decline in inertia and grid strength. While this remains a pressing challenge for the power system, the integration of advanced power electronic control algorithms has alleviated the issue through the adoption of GFM technologies [2], systems that can emulate the dynamic behavior of synchronous generators. In this regard, battery energy systems are particularly suited for GFM emulation. Their stable DC link can enable bidirectional responses to both frequency and voltage deviations, making them a key asset for enhancing the network stability and resilience [3]. Many concerns are arising on the interoperability of systems, especially with the integration of GFM on PV assets, since operational discrepancies across devices may amplify interactions, leading to uncontrolled oscillations and possibly to unintended power exchanges across the distribution network [4].

Transient angle and voltage stability have risen as very specific concerns for grid-connected power electronic assets. The effect of grid disturbances to the phase angle of the converter can lead to loss of synchronization on the unit which is then more prone to a potential cascaded fault causing partial or total blackouts on the electrical network. In [5] GFM devices are analyzed with reactive and active power controllers, pointing out the potential instability of such converters on the electrical network. This paper aims to analyze the impact of GFM into distribution grids by analyzing the impedance behavior of a singular unit to later analyze its behavior in a multi-GFM distribution network with different short circuit ratios (SCR). Finally, the GFM functionality is analyzed together with typical tap changer interactions and final recommendations for DSO deployment are presented. This paper is structured as follows: Section 2 presents the standard GFM converter control with parameters and key understanding of its behavior. Section 3 focuses on the definition of the site under analysis and the different units connected to the whole system and shows the analysis of the system on different test cases, giving insights about the operation of the system under different penetration of GFM renewable assets. Finally, section 4 presents the overall conclusions of the paper and highlights its contributions.

2. Grid-Forming Control

Conventional synchronous power plants inherently provide grid stability through their rotating masses, which supply inertia, maintain voltage, and establish system frequency as part of the electromechanical dynamics of the machine. Their control is relatively slow but naturally coordinated, as frequency and voltage emerge from the physical coupling of generators. In contrast, converters equipped with grid-forming controllers emulate these stabilizing properties through fast control algorithms rather than standard mechanical inertia [6]. They can establish voltage and frequency in weak or inverter-dominated grids, respond much faster to disturbances, and be flexibly tuned for different operating conditions. However, unlike synchronous machines, GFMs require careful parameter design, coordination, and protection schemes to ensure stable interaction with other resources. This makes them more versatile and flexible, but also more complex to deploy and integrate at large scale. For instance, adverse interactions between grid-forming units have been observed in the field, which are still not very well understood as shown in [4]. Moreover, their characteristics in terms of overcurrent are much more limited than in conventional units [7].

While the implementation of grid-forming control for type D systems directly connected to the 110 kV grid may be more straightforward, this was not the focus of the original investigations. Instead, the studies concentrated on the integration of grid-forming control into local low-voltage distribution networks. The findings indicate that grid-forming technology offers promising capabilities for stabilizing converter-dominated grids. However, its deployment at the distribution level introduces several challenges. Key concerns include personnel safety due to unintended islanding and the adaptation of protection schemes. The additional short-circuit power introduced by grid-forming inverters may not always be beneficial and the technology can lead to unintended islanding and controller oscillations, potentially compromising system stability and operational reliability. From the perspective of distribution system operators (DSOs), grid-forming control can help mitigate voltage issues in weak grids or areas with high photovoltaic penetration. It also enables functionalities such as islanded operation and black start capability, nevertheless the island operation is only partially practical in real-world distribution networks and require further validation.

One of the most common strategies of a GFM system is the one using a power synchronization loop. This synchronization loop enables the converter with inherent inertial response due to the synchronization factor with the mechanical behavior of the swing equation. This behavior produces a natural interconnection to the electrical network that defines the operation point of the active power setpoint. For the reactive power setpoint, the internal electromotive force can be used to regulate the amount of reactive power exchanged to the network. The equipment of an additional droop control enables the power converter to inject power into the electrical network in the same way as a grid-following would do, presenting a very standard regulation system on the grid-forming converter. The most typical control structure can be represented as in Figure 1, which is composed of 4 core parts: the inner current controller, the virtual impedance/admittance, the active power regulation and the reactive power regulation.

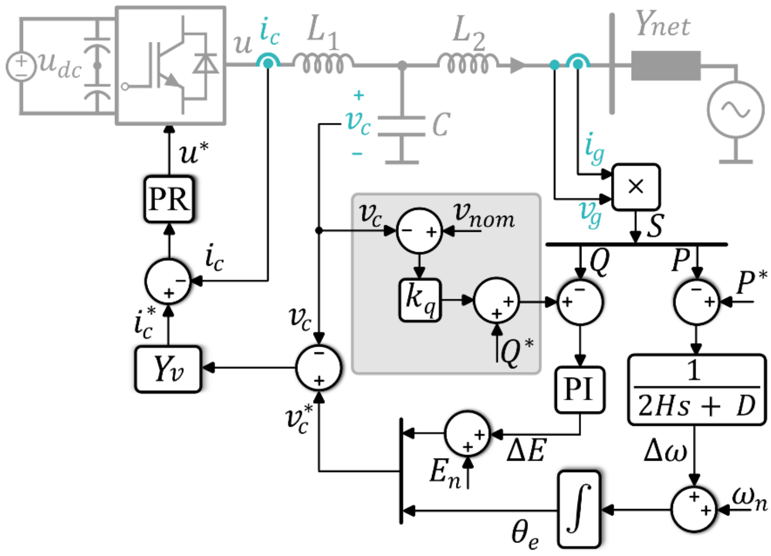

Figure 1. *Power converter control of a grid-forming power converter.*

Each of these loops is key to maintaining the power converter under normal operation connected to the grid. The inner loops, current control and virtual admittance are pivotal for the stable operation of the converter. As a standard implementation, Figure 1 showcases the current controller as a proportional-resonant (PR) system (1):

$$PR(s) = k_p + \frac{2k_i}{s^2+\omega_n^2} \quad (1)$$

Were the k_p and k_i parameters play a key role on the stability on the converter, especially when operating on island or ultra weak grid conditions. In the case of virtual admittance (VA) the system uses an equivalent inductance, L_v, and a resistance, R_v, which are in charge of creating the needed current reference for the inner current controller. Those parameters can be dynamically modified during operation to change the X/R relation at the output of the power converter.

$$Y_v(s) = \frac{1}{L_v s+R_v} \quad (2)$$

At the input of the virtual admittance block, the error of the internal electromotive force and the actual voltage measured at the PCC of the power converter plays a crucial role in determining the amount of support provided by the unit towards the grid stability. On the one side, the swing equation structure, used as the active power control, has been widely used to emulate synthetic inertial response from a power converter due to its native inertial capability [6]. This structure, (3), can be tuned using its internal parameters H and D to adjust the amount of inertial response and damping capacity that the converter is emulating.

$$G_P(s) = \frac{1}{2Hs+D} \tag{3}$$

Moreover, reactive power control is in charge of maintaining the magnitude of the internal electromotive force, E, of the power converter. This is achieved by a simple proportional or a PI regulator that compensates for the voltage drop to maintain the same voltage magnitude as the grid to ensure reactive power transfer, (4). The parameters to tune the speed of this regulation system depend on the integral gain, k_i, and the proportional gain, k_p.

$$G_Q(s) = \frac{k_p s+k_i}{s} \tag{4}$$

This effect can be used when no reactive power exchange is necessary, however it also disables the capacity of the GFM to operate in standalone islanded operation. To avoid this, in most of the GFM solutions a reactive power droop system is implemented. This structure allows for deadband implementation and is usually a settable gain, k_q, to allow for a maximum voltage drop of 20% of the voltage to provide nominal reactive power towards the grid.

$$\Delta Q = (v_{nom} - v_c) \cdot k_q \tag{5}$$

2.1 Small Signal analysis of GFM

The control in Figure 1 can be represented based on the transfer functions defining the GFM control structure. In this case, this model can be then used for small signal analysis to study the stability and performance is presented in Figure 2.

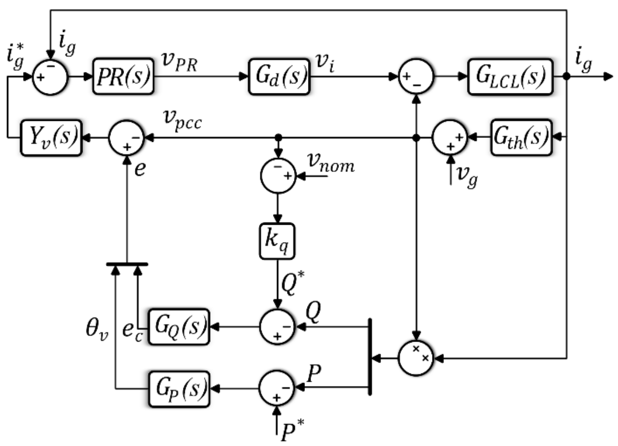

Figure 2. *Small signal model of a standard GFM power converter*

This small signal structure is composed of the same blocks presented in section 2 and the linearized blocks for the pulse-width modulation (PWM) inverter switching stage, as well as the physical LCL output filter of the converter and the grid impedance represented by the transfer function $G_{th}(s)$, that allows for studying the system with different grid-strength on the distribution network [8].

In order to approximate the effect of the switching stage of the power converter, a second order padé approximation is used to rationalize the delay factor.

$$G_d(s) = \frac{12-6T_d s+T_d^2 s^2}{12+6T_d s+T_d^2 s^2} \quad (6)$$

This enables the derivation of the small-signal model as the system can be linearized around the operating point. Power converters are closely tied to their inherent impedance characteristic, which can describe how the converter will interact to the electrical network. The small signal structure is used to characterize that output impedance behaviour and highlight each controller effect on the structure, as show in Figure 3. It is possible to see in this figure two key points, on the one hand Figure 3(a) displays the admittance on the main diagonal matrix, presenting the admittance behaviour $Y_{\alpha\alpha}$ or $Y_{\beta\beta}$ of the power converter. In this case, the high gain at the lower frequencies can massively increase the response of the converter to DC quantity existing on the electrical network, which can harm other assets connected on the same network if not properly handled [9]. In terms of the active and reactive power controllers, they only have effect close to the nominal frequency, also called positive sequence, where the power can be exchanged to the electrical network. At around 7kHz, the system is presenting a high resonance value defined by its LCL structure together with the current control. This high frequency resonance can be excited on the power converter if the grid presents some high frequencies perturbation on the voltage, which has already occurred in some heavy harmonic resonance around Europe.

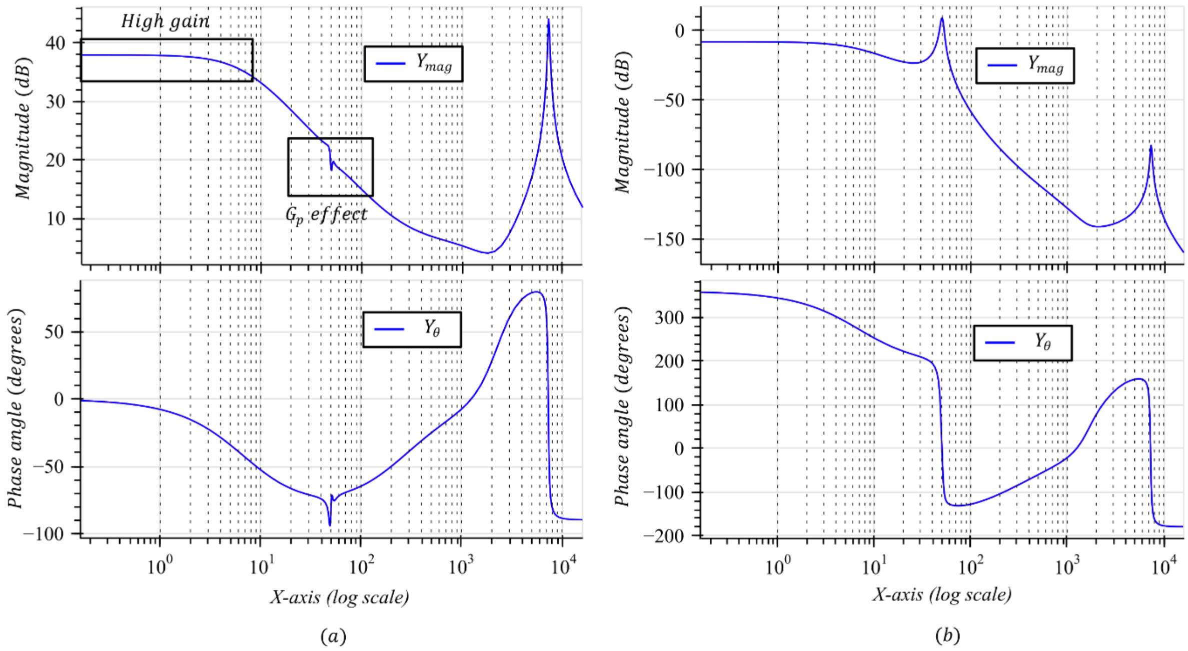

Figure 3. *Impedance response of a GFM connected to the grid, components* $\boldsymbol{Y_{\alpha\alpha}}$ **and** $\boldsymbol{Y_{\alpha\beta}}$ *for a very strong grid interconnection. (a)* $\boldsymbol{Y_{\alpha\alpha}}$ *magnitude and phase angle. (b)* $\boldsymbol{Y_{\alpha\beta}}$ *magnitude and phase angle.*

Even though Figure 3 shows that the system would be stable as it maintains the main diagonal, $\boldsymbol{Y_{\alpha\alpha}}$, phase angle between -90 and +90 degrees, and the virtual resistance ensures that the system do not present non-negative real parts on the impedance, the grid strength does affect a lot on the overall system stability. The active power controller, Gp(s), only has effect on the nominal frequency of the converter, which is highlighted in Figure 3. To mitigate some of the disturbances at low frequencies (300-1000Hz) a voltage feedforward structure is usually integrated to accelerate the converter response in case of faults and other grid transients, see Figure 4. Even though it has been proven that the feedforward plays a crucial role in transient behavior of the power converter especially considering faults, it also heavily increases the resonances appearing on the output of the converter that can lead to voltage and frequency oscillations. This phenomenon can be further evaluated at different SCR, where the lower SCR reduces the stability of the feedforward term on the voltage stability.

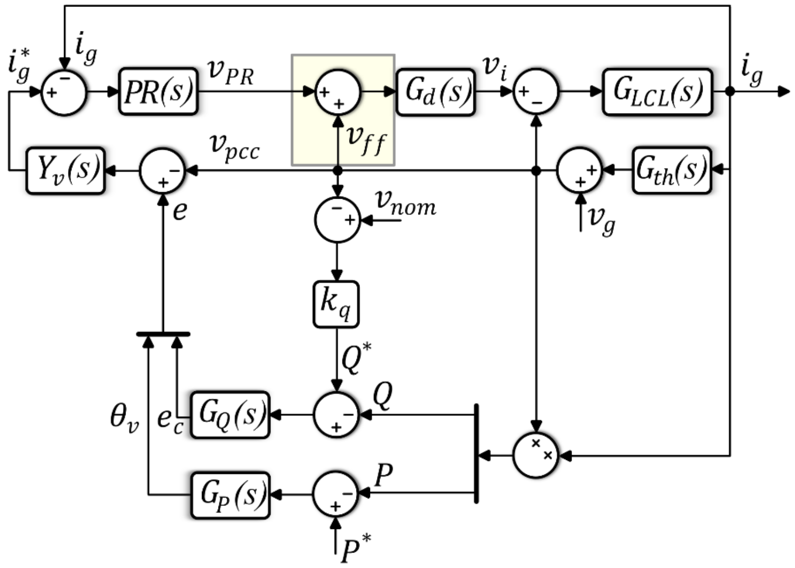

Figure 4. *Small signal model of a standard GFM power converter using voltage feedforward term on the output control voltage.*

It is possible to see in Figure 5(a) how the impedance response at different frequencies is modified. It is worth highlighting that the response from very high SCR 100 to a value of 10 does not massively change the impedance shape through the whole frequency spectrum, except that the resonance frequency of the LCL filter comes closer to the 2kHz. However, when the SCR of the grid decreases to an ultra-weak grid the response of the impedance through the whole structure is reduced in gain, thus affecting not only the DC gain at low frequencies but also eliminating the resonance effect of the LCL filter. On the other side, Figure 5(b) showcase the effect of the voltage feedforward on the structure at different SCRs. It is possible to see from the image that the LCL resonance peak comes closer to the low frequency range, shifting from almost 7kHz to a value below 1kHz. This performance is critical for ultra-weak grid systems.

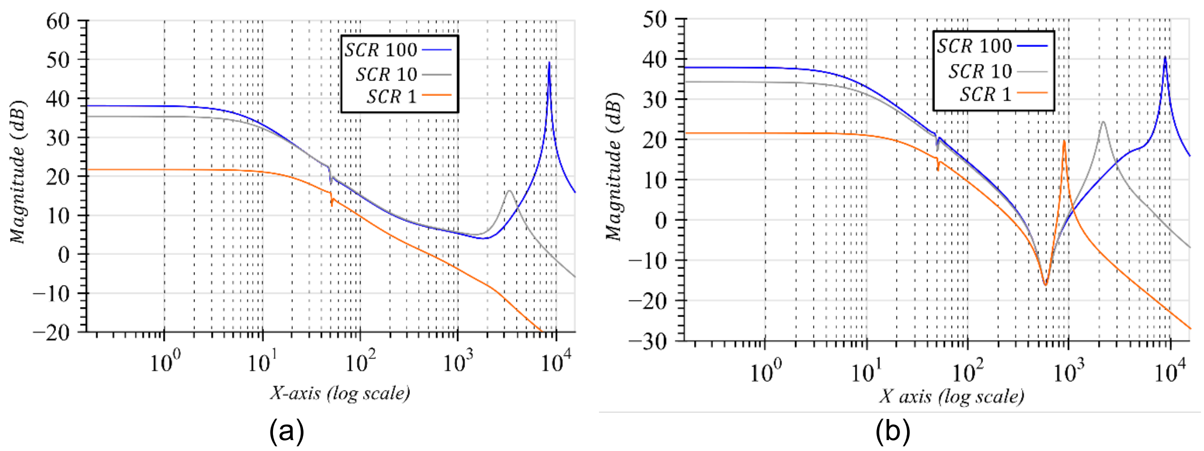

Figure 5. *Impedance response of a GFM, gain for* $\boldsymbol{Y}_{\alpha\alpha}$*.(a) without feedforward (b) with feedforward matrix.*

3. Location selection for analysis

The integration of grid-forming units demands new protection concepts, control logic, and clear regulatory guidelines. Moreover, the coordination of such units remains an open question: should individual DSOs be responsible, or should this fall under the remit of a central system operator? The procurement of grid-forming services also requires clarification, whether through market-based mechanisms or predefined obligations in grid codes. Both platform-based and tender-based models are currently under discussion, each with implications for transparency, efficiency, and long-term planning. In this paper a methodological approach is used for the analysis and impact of grid-forming into specific distribution network areas. The analysis deals with the stability of the power converter interactions at different points of the network to determine its impact on the distribution level. The selected areas are shown in Figure 2(a) and Figure 2(b). In addition, the positive influence of grid-forming on the PCC voltage within the grid sections is being investigated.

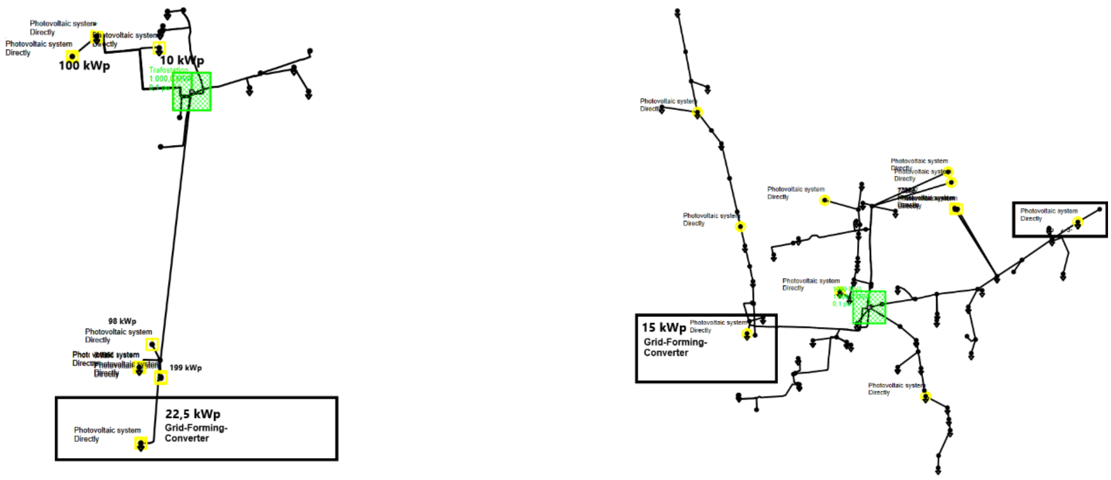

(a) (b)

Figure 6. *Distribution network (a) low-voltage network with industrial consumers and high PV density (b) typical low-voltage network with households (PSS Sincal + Matlab - Simplus Grid Tool)*

To assess the stability of the grid-forming functionality different test cases have been considered, different load scenarios, different grid strength and different X/R ratios.

3.1 Integration analysis of GFM into the distribution network

To validate the operation of the GFM unit, different scenarios were planned to evaluate its behavior under different penetration levels of GFM and different grid operating points. The model used for analysis is the translated model from Figure 6, originally in PSS Sincal, to Matlab – Simplus Grid Tool to evaluate the performance of multiple GFMs on the grid. All the tested cases are presented in Table 1, where multiple combinations of GFM and GFL units based on 5 grid-connected units, different SCR and X/R ratio were used during performance analysis. It is worth mentioning that over all the cases, all the GFM units were stable and could operate interconnected to other devices in the electrical network. In all cases the distribution of GFM and GFL was set to 1 and 4 respectively, except for test case 10, which is the one under test in this section where all units are replaced by GFM units.

Table 1. *Test validation cases of the GFM under an industrial distribution network with high PV density.*

Test num	Description	Grid SCR	Grid R/X	Operating point
1	Nominal powers	1000	0.33	P=1, Q=0.0382, V=1.0595,
2	Negative setpoint on conv.	1000	0.33	P=-1, Q=0, V=1.0475
3	Load set to zero	1000	0.33	P=1, Q=0.3558, V=1.1389
4	Prod PV to zero	1000	0.33	P=0, Q=-0.2479, V=0.8880
5	Nominal powers	100	0.33	P=1, Q=0.1040, V=1.076
6	Reduced powers	10	0.33	P=1, Q=0.0, V=1.0059
7	Reduced powers	1	0.33	P=1, Q=0.0, V=0.9869
8	Nominal powers	100	1	P=1, Q=0.2599, V=1.1150
9	Nominal powers	100	3	P=1, Q=0.3666, V=1.1416
10	All grid forming	100	1	P=1, Q=0.0, V=1.0059

To showcase the GFM performance of the different grid forming units, selected test cases are presented in the paper. The locations of the different units are on the yellow dots in Figure 6 and the grid selected for the results in grid (a). First, the dynamic response of 5 GFM units under a phase jump on the electrical network of 10 degrees will highlight the dynamic support provided by the system. Second, synthetic inertia will be showcased with a rate of change of frequency (RoCoF) of 0.5Hz/s on the network. Finally, a sudden voltage step will be analyzed comparing the reactive power support towards the electrical network. The differences in all the units are due to the line impedance existing on the network in Figure 6.

It is possible to see in Figure 7 that when a sudden change on the phase angle of the electrical network occurs the virtual impedance and the synchronization loop on the GFM converter try to adapt to the new phase angle setpoint. During this time, the system is able to provide additional power to the network to mitigate the phase jump. Even though a 10-degree phase jump is substantial on the grid voltage, all the grid forming are able to maintain stability while providing the necessary amount of energy to the network.

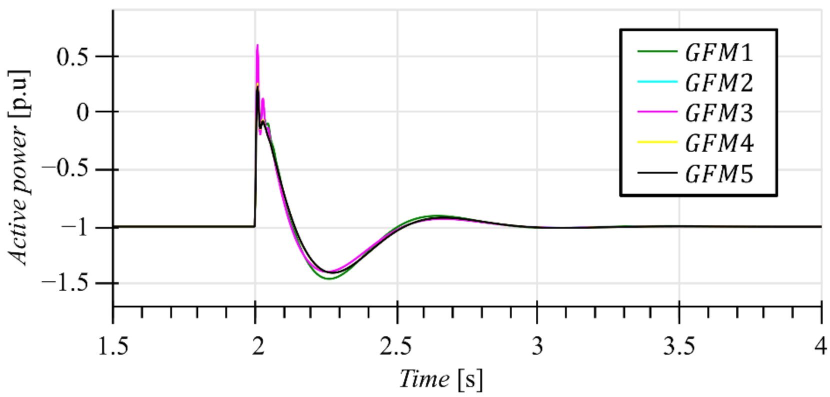

Figure 7. *Phase jump of 10º on the grid voltage with a strong grid.*

To demonstrate synthetic inertia provision, Figure 8 highlights the effort from multiple GFM units during a RoCoF event of 0.5Hz/s. By definition, the amount of power needed to be exchanged towards the electrical network due to synthetic inertia constant is dependent on the derivative term of the frequency. Following that, the system is able to inject constant power during a specific RoCoF on the network. In this case, all the power converters are set to have the same amount of impedance and synthetic inertia provision, so all the power converters reduce their power injection from 1 p.u to 0.73 p.u. After the RoCoF get into a steady state value, that static power exchanged towards the grid from the power converter is resumed and the converter goes back to its previous setpoint.

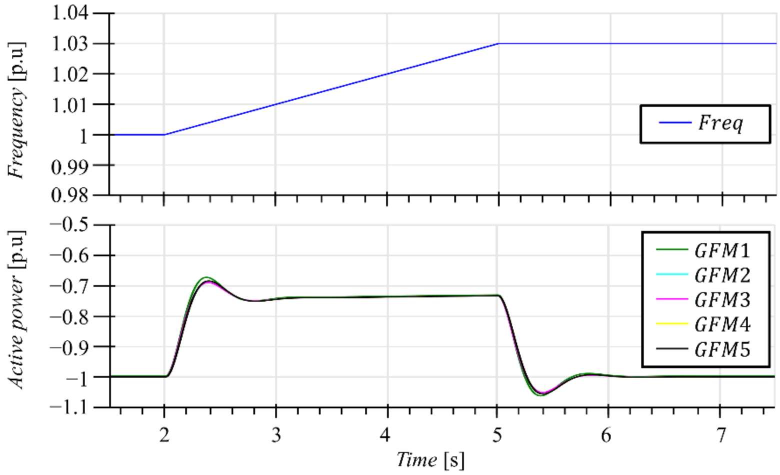

Figure 8. *Rate of change of frequency of 0.5Hz/s.*

Finally, during a voltage sag or a sudden change on the voltage amplitude of the grid voltage the GFM power converters should provide an amount of inductive reactive power to increase the voltage at its point of connection to the maximum extent possible dependent on the grid strength. It is possible to see from Figure 9 that during a sudden change in the voltage magnitude at the point of common coupling (PCC), the GFM units dynamically react to that change due to their natural characteristic. Thanks to the virtual impedance, the system is able to inject a controlled reactive power reference that is able to increase the PCC voltage. The differences in the amount of reactive power injected by each power converter depends on the line impedance and the actual voltage seen by the power converter at its own PCC.

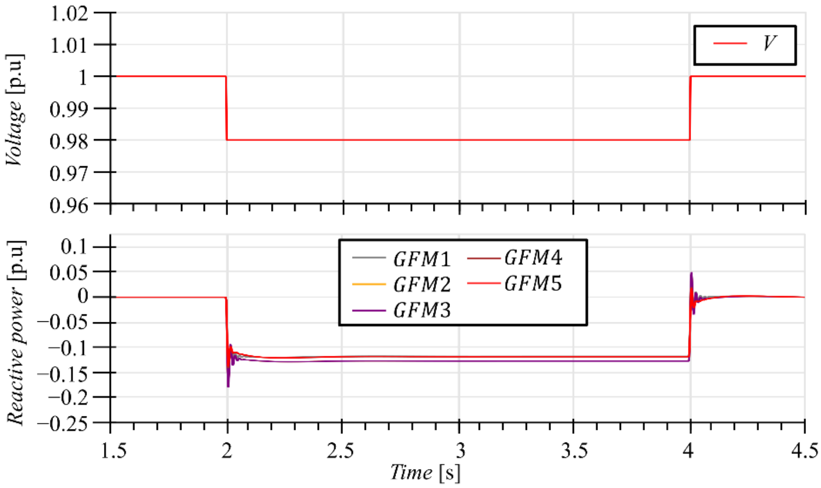

Figure 9. *Sudden voltage step at the grid from 1 to 0.98 p.u.*

3.2 GFM stability interconnected through a transformer with tap changer.

One of the challenges of GFMs in distribution grids is the possible adverse interactions with other components that may be in charge of regulating voltage levels, such as tap changers. In this sub-section a verification of the stable operation of the GFM unit when interconnected to the main grid through a tap changer transformer is presented, see Figure 10. In order to analyse whether the voltage regulator of the GFM and the tap changer would fight each other, different gains and tap parameters were explored. It was observed that the GFM controller was never leading to instability, and only in the case of an ill-designed tap changer, oscillations would occur. In order to see this behavior, two cases have been selected where different operating points for the tap changer were selected: on one case the tap changer was stable and was regulating the voltage at the load side of the transformer. On the other case, the system was already having an unstable behavior of the tap changer prior to the connection of the grid forming to the network.

Table 2. *Tap changer control parameters on the stable and unstable case.*

Stable Case	Unstable case
delay_tapChanger = 0.15 s	delay_tapChanger = 0.3 s
deadband_tapChanger = 0.05 s	deadband_tapChanger = 0.01 s

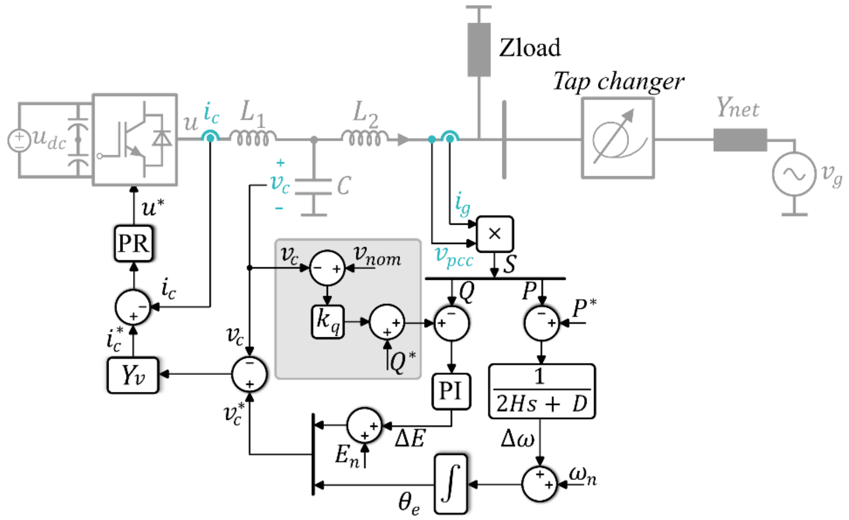

Figure 10. *Power converter control of a grid-forming power converter interconnected through a transformer with tap changer.*

It is possible to see in Figure 11(a) that after the connection of the grid forming the system is able to recover the voltage close to 1 p.u value as the system is able to slowly inject reactive power to support the voltage at the grid side. After the load connection at t= 5s, the tap changer is able to increase the voltage at the load side meanwhile the GFM unit is also trying to stabilize the voltage. Indeed, rather than interacting adversely, the GFM is contributing towards voltage regulation. In Figure 11(b), the tap changer was already having voltage oscillations prior to the GFM connection to the network. After the GFM is connected, the system stabilized two seconds before the load connection at t=5s. After the load connection the tap changer try to regulate the voltage at the load side, however, its inherent unstable operation keeps working and the GFM is unable to stabilize it.

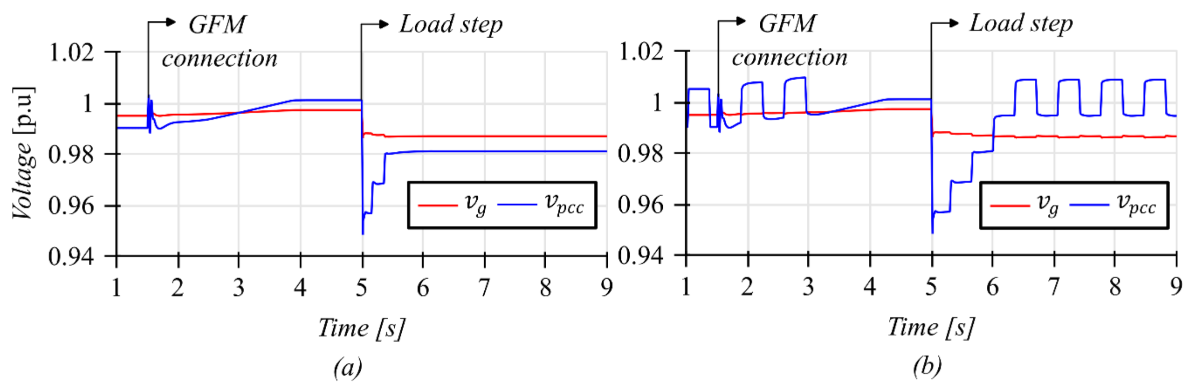

Figure 11. *GFM with a tap changer transformer interaction. (a) stable tap changer case with GFM. (b) unstable tap changer case with GFM.*

4. Conclusion

This paper has presented a detailed, step-by-step examination of GFM control within the distribution network environment. Beginning with a small-signal analysis of a standard GFM control algorithm, the study demonstrated the inherent stability and performance benefits of GFM operation across a wide range of operating conditions. The analysis also highlighted implementation details, particularly in the use of voltage feedforward, that can introduce undesired oscillations or resonances under weak-grid conditions, a frequent scenario in microgrid or remote locations. A second contribution is the comprehensive assessment of GFM behavior in a real industrial environment. Multiple test cases, encompassing converters with different SCR, X/R ratios and active/reactive power setpoints, were thoroughly evaluated. Across all the scenarios the GFM units consistently operated in a stable fashion and provided the required powers support to the electrical network when demanded. The paper further explored the interaction between GFM converter and on-load tap changer transformers. The results indicate that GFM technology does not inherently destabilize grids equipped with tap changers. In cases where instability was observed prior to the GFM connection, the system remained prone to an unstable behavior even when connecting the GFM unit. Overall, the simulation results presented in this study cover a wide spectrum of practical operating conditions, reinforcing the robustness and suitability of GFM control for modern distribution networks.

Author contributions

Andres Tarraso: Identifying issues on grid-forming solutions, fundamental small-signal analysis.

Maximilian Prasser: Definition of the grid under study.

Adolfo Anta: Developing simulation results.

Competing interests

The authors declare that they have no competing interests.

Funding

The research in this study has been carried out within the frame of cells4.energy project (https://projekte.ffg.at/projekt/4849884) and funded by Austrian Research Promotion Agency

(Österreichische Forschungsförderungsgesellschaft, FFG) under the grant agreement number 904664.

References

[1] "Renewables 2025 Global Status Report - REN21."
[2] P. Rodríguez, C. Citro, J. I. Candela, J. Rocabert, and A. Luna, "Flexible Grid Connection and Islanding of SPC-Based PV Power Converters," *IEEE Trans. Ind. Appl.*, vol. 54, no. 3, pp. 2690–2702, 2018, doi: 10.1109/TIA.2018.2800683.
[3] "RELIABILITY | RESILIENCE | SECURITY NERC | Report Title | Report Date I White Paper: Grid Forming Functional Specifications for BPS-Connected Battery Energy Storage Systems," 2023.
[4] R. Denninger *et al.*, "Case study: interoperability of two independently designed grid-forming converters," in *23rd Wind & Solar Integration Workshop (WIW 2024)*, 2024, pp. 274–280. doi: 10.1049/icp.2024.3799.
[5] W. Si, J. Fang, X. Chen, T. Xu, and S. M. Goetz, "Transient Angle and Voltage Stability of Grid-Forming Converters With Typical Reactive Power Control Schemes," *IEEE J. Emerg. Sel. Top. Power Electron.*, vol. 13, no. 3, pp. 2917–2927, 2025, doi: 10.1109/JESTPE.2024.3477492.
[6] W. Zhang, A. Tarraso, J. Rocabert, A. Luna, J. I. Candela, and P. Rodriguez, "Frequency Support Properties of the Synchronous Power Control for Grid-Connected Converters," *IEEE Trans. Ind. Appl.*, vol. 55, no. 5, pp. 5178–5189, 2019, doi: 10.1109/TIA.2019.2928517.
[7] O. Stanojev, O. Karaca, and M. Schweizer, "Grid-forming vector current control FRT modes under symmetrical and asymmetrical faults," *Sustainable Energy, Grids and Networks*, vol. 43, Sep. 2025, doi: 10.1016/j.segan.2025.101830.
[8] Z. Zou, Z. Wang, and M. Cheng, "Modeling, Analysis, and Design of Multifunction Grid-Interfaced Inverters With Output LCL Filter," *IEEE Trans. Power Electron.*, vol. 29, no. 7, pp. 3830–3839, 2014, doi: 10.1109/TPEL.2013.2280724.
[9] D. Cifelli, A. Tarraso-Martinez, and M. Prasser, "Harmonic Modelling of a Grid-Forming Inverter in Stationary Frame," in *IECON 2025 – 51st Annual Conference of the IEEE Industrial Electronics Society*, 2025, pp. 1–6. doi: 10.1109/IECON58223.2025.11221471.